Polyhedron 87 (2015) 17–27

Contents lists available at ScienceDirect

Polyhedron

journal homepage: www.elsevier.com/locate/poly

Metal derivatives of N-substituted imidazolidine-2-thiones with d^{10} metal ions (Zn–Hg): Synthesis, spectroscopy, ESI-mass and structures

Tarlok S. Lobana [a,*], Amanpreet K. Sandhu [a], Amanpreet K. Jassal [a], Geeta Hundal [a], R.K. Mahajan [a], Jerry P. Jasinski [b], Ray J. Butcher [c]

[a] Department of Chemistry, Guru Nanak Dev University, Amritsar 143 005, India
[b] Department of Chemistry, Keene State College, Keene, NH 03435-2001, USA
[c] Department of Chemistry, Howard University, Washington, DC 20059, USA

A R T I C L E I N F O

Article history:
Received 7 July 2014
Accepted 7 October 2014
Available online 25 October 2014

Keywords:
N-methyl-imidazolidine-2-thione
N-ethyl-imidazolidine-2-thione
N-*n*-propyl-imidazolidine-2-thione
Zinc
Cadmium

A B S T R A C T

N-substituted 1,3-imidazolidine-2-thiones (L^{I}-NMe; L^{II}-NEt; L^{III}-NPr^{n}) on reacting with Zn(II), Cd(II) and Hg(II) halides in methanol have yielded the mononuclear complexes $[ZnCl_2(L^{II}\text{-NEt-}S)_2]$ **1**, $[ZnI_2(L^{I}\text{-NMe-}S)_2]$ **2**, $[CdBr_2(L^{I}\text{-NMe-}S)_2]$ **3**, $[CdBr_2(L^{II}\text{-NEt-}S)_2]$ **4**, $[CdI_2(L^{I}\text{-NMe-}S)_2]$ **5**, $[HgCl_2(L^{I}\text{-NMe-}S)_2]$ **6**, $[HgCl_2(L^{III}\text{-NPr}^{n}\text{-}S)_2]$ **7** and $[HgI_2(L^{I}\text{-NMe-}S)_2]$ **8**. All these complexes have been characterized by elemental analysis, spectroscopy (IR, ^{1}H NMR), ESI-mass and X-ray crystallography. Complexes **1**–**6** and **8** crystallized in the monoclinic system, with each having the space group $P2_1/c$ except for complex **4** which has the space group $C2/c$, and complex **7** crystallized in the trigonal system with the space group $R\text{-}3c$. Interestingly, the complex molecules adopt four types of conformations which give rise to different patterns of intermolecular interactions and hence 2D (**1**–**6**, **8**) or 1D (**7**) polymeric networks are obtained. ESI mass data support the formation of $[M{-}X]^{+}$ ions (X = halogen) in complexes **1**–**7**.

1. Introduction

The coordination chemistry of heterocyclic thiones has invited the attention of many research workers over the past four decades, as revealed by several reviews in this area [1–5]. These thio ligands have the propensity to coordinate to a metal as a neutral ligand or as an anionic ligand. Due to the presence of the soft sulfur donor atom in the vicinity of the nitrogen atom in the heterocyclic ring, these thio ligands exhibit several types of coordination modes [1–16]. Among these heterocyclic thiones, 1,3-imidazolidine-2-thione and its N-substituted derivatives (Chart 1) have formed mononuclear, dinuclear and polynuclear complexes with coinage metals (Cu–Au) [17–33], and post transition metals (Zn–Hg) [34–38,18,39–43]. In addition, these ligands with copper salts have displayed interesting chemical reactivity, such as C–S rupture with the in situ formation of sulfate and a new type of reaction products [15,16].

Recently, coordination compounds of post transition metals (Zn, Cd, Hg) with 1,3-imidazolidine-2-thione (L^{IV}-NH, R = H, Chart 1) have been reported from this laboratory [43]. In the literature, the number of compounds of post transition metals (Zn, Cd, Hg) reported with substituted imidazolidine-2-thiones [36,37,40] are relatively less as compared to 1,3-imidazolidine-2-thione complexes [34,35,38,18,39,41–43]. It may be noted that there are a few reports on the biological properties of 1,3-imidazolidine-2-thione (L^{IV}-NH) complexes with Zn^{II} and Cd^{II}, but none with Hg^{II} [36,37]. It is noted that a complex of 1,3-imidazolidine-2-thione with Zn^{II} has shown higher biological activity against *Pseudomonas aeruginosa* and *Escherichia coli* than its Cd^{II} analog [36]. In this paper, the coordination compounds of Zn^{II}, Cd^{II} and Hg^{II} with N-substituted 1,3-imidazolidine-2-thiones (L^{I}-NMe; L^{II}-NEt; L^{III}-NPr^{n}) (Chart 1) are reported so as to provide a status report on the coordination chemistry of Zn–Hg metals with the thio ligands under study.

2. Experimental

2.1. Materials and techniques

The thio ligand 1-methyl-imidazolidine-2-thione (L^{I}-NMe) was prepared by the addition of carbon disulfide dropwise to a cooled solution of 1-methyl-ethylenediamine in ethanol and water. The reaction mixture was heated under reflux (110 °C) for 1 h and conc. HCl was added. The mixture was heated under reflux for a further period of 10 h. The reaction mixture was cooled and stored in a freezer. The resulting precipitate were filtered and washed with

---

[*] Corresponding author. Tel.: +91 183 2258802x3195; fax: +91 183 2258820.
E-mail address: tarlokslobana@yahoo.co.in (T.S. Lobana).

http://dx.doi.org/10.1016/j.poly.2014.10.016
0277-5387/

cold acetone to give the desired ligand. In a similar manner, 1-ethyl-imidazolidine-2-thione (L^{II}-NEt) and *n*-propyl-imidazolidine-2-thione (L^{III}-NPr^n) were prepared [44]. The metal salts {ZnX_2 (X = Cl, I), CdX_2 (X = Br, I) and HgX_2 (X = Cl, I)} were procured from Spectrochem Pvt. Ltd. The melting points were determined with a Gallenkamp electrically heated apparatus. The IR spectra were recorded using KBr pellets on Varian 660 FT IR and Perkin Elmer FT IR spectrometers in the 4000–200 cm^{-1} range. The ^1H NMR spectra were recorded in $CDCl_3$ using a Bruker Avance II 400 NMR spectrometer at 400 MHz and a JEOL AL300 FT ^1H NMR spectrometer at 300 MHz using TMS as an internal reference. The ESI-MS mass spectrometer used was a microTOF-QII 10356 in the positive mode.

2.2. Synthesis of the complexes

2.2.1. Synthesis of [$ZnCl_2$(L^{II}-NEt-S)$_2$] (**1**)

To a solution of 1-ethyl-imidazolidine-2-thione (0.047 g, 0.362 mmol) in methanol (5 mL) was added a solution of zinc(II) chloride (0.025 g, 0.183 mmol) in methanol (5 mL). The reaction mixture was stirred for 2 h at room temperature. To this mixture was added dichloromethane (5 mL) and then slow evaporation at room temperature formed colorless crystals of **1** (70%, m.p. 155–157 °C). *Anal.* Calc. for $C_{10}H_{20}Cl_2N_4S_2Zn$: C, 30.28; H, 5.08; N, 14.12. Found: C, 30.22; H, 5.01; N, 14.02%. IR bands (KBr, cm^{-1}) : ν(N–H) 3244 s; ν(C–H) 3025 w, 2977 m, 2934 m, 2888 m; ν(C–C) + ν(C–N) + δ(C–H) 1516 s, 1479 m, 1460 m; 1381 m, 1358 w, 1341 w, 1324 m, 1209 s, 1269 s, 1203 w; ν(C–S) 1127 s; 1079 m, 976 w, 951 m, 794 m, 649 w, 620 m, 586 s, 506 s. ^1H NMR data ($CDCl_3$, δ ppm): 8.42 (s, 2H, NH), 3.72 (m, 8H, $C^{4,5}H$), 3.57 (m, 4H, N-CH_2), 1.20 (t, 6H, *J*, 7.2 Hz, CH_3). ESI-mass data, calc. for $[M-35]^+$, formula {$C_{10}H_{20}ClN_4S_2Zn$}, *m*/*z*: 359.0; observed *m*/*z*: 359.0.

2.2.2. Synthesis of [ZnI_2(L^I-NMe-S)$_2$] (**2**)

To a solution of 1-methyl-imidazolidine-2-thione (0.018 g, 0.155 mmol) in methanol (5 mL) was added a solution of zinc(II) iodide (0.025 g, 0.078 mmol) in methanol (5 mL). The reaction mixture was stirred for a period of 2 h at room temperature and a white precipitate was formed. To the precipitate was added dichloromethane (5 mL) and methanol (5 mL). Slow evaporation at room temperature formed colorless crystals of **2** (70%, m.p. 158–160 °C). *Anal.* Calc. for $C_8H_{16}I_2N_4S_2Zn$: C, 17.45; H, 2.75; N, 10.18. Found: C, 17.58; H, 2.68; N, 10.15%. IR bands (KBr, cm^{-1}): ν(N–H) 3307 s; ν(C–H) 2919 w, 2890 w; ν(C–C) + ν(C–N) + δ(C–H) 1541 s, 1508 s, 1469 m, 1401 m; 1325 s, 1300 s, 1288 s, 1194 m; ν(C–S) 1111s; 1022 m, 955 w, 633 m, 504 s. ^1H NMR data ($CDCl_3$ + [D_6]DMSO, δ ppm): 7.04 (s, 2H, NH), 3.73 (m, 8H, $C^{4,5}H$), 3.14 (m, 6H, CH_3). ESI-mass data, calc. for $[M-127]^+$, formula {$C_8H_{15}IN_4S_2Zn$}, *m*/*z*: 421.9; observed *m*/*z*: 422.9.

2.2.3. Synthesis of [$CdBr_2$(L^I-NMe-S)$_2$] (**3**)

To a solution of 1-methyl-imidazolidine-2-thione (0.021 g, 0.181 mmol) in methanol (5 mL) was added a solution of cadmium(II) bromide (0.025 g, 0.092 mmol) in methanol (5 mL). The reaction mixture was stirred for a period of 2 h at room temperature and a white precipitate was formed. To the precipitate was added dichloromethane (5 mL) and methanol (5 mL). The slow evaporation at room temperature formed colorless crystals of **3** (76%, m.p. 148–150 °C). *Anal.* Calc. for $C_8H_{16}Br_2CdN_4S_2$: C, 19.03; H, 3.02; N, 11.10. Found: C, 8.87; H, 3.06; N, 11.21%. IR bands (KBr, cm^{-1}): ν(N–H) 3294 s; ν(C–H) 2921 w, 2892 w; ν(C–C) + ν(C–N) + δ(C–H) 1543 s, 1510 s, 1470 m, 1403 w; 1329 m, 1219 s, 1198 m; ν(C–S) 1113 s; 1026 w, 959 w, 635 m, 541 m, 504 m. ^1H NMR data ($CDCl_3$ + [D_6]DMSO, δ ppm): 7.75 (s, 2H, NH), 3.67 (m, 8H, $C^{4,5}H$), 3.07 (m, 6H, CH_3). ESI mass data, calc. for $[M-79]^+$, {$C_8H_{16}BrCdN_4S_2$} *m*/*z*: 424.9; observed *m*/*z*: 423.2.

2.2.4. Synthesis of [$CdBr_2$(L^{II}-NEt-S)$_2$] (**4**)

To a solution of 1-ethyl-imidazolidine-2-thione (0.0235 g, 0.181 mmol) in methanol (5 mL) was added a solution of cadmium(II) bromide (0.025 g, 0.092 mmol) in methanol (5 mL). The reaction mixture was stirred for 2 h at room temperature and slow evaporation at room temperature formed colorless crystals of **4** (71%, m.p. 118–120 °C). *Anal.* Calc. for $C_{10}H_{20}Br_2CdN_4S_2$: C, 22.55; H, 3.78; N, 10.52. Found: C, 22.20; H, 3.75; N, 10.58%. IR bands (KBr, cm^{-1}): ν(N–H) 3250 s; ν(C–H) 2971 m, 2927 m, 2881 m; ν(C–C) + ν(C–N) + δ(C–H) 1515 s, 1453 m; 1380 w, 1321 m, 1266 s; ν(C–S) 1123 s; 1077 w, 1031 w, 949 w, 791 w, 619 m, 550 m, 502 m. ^1H NMR data ($CDCl_3$, δ ppm): 7.95 (s, 2H, NH), 3.76 (m, 8H, $C^{4,5}H$), 3.61 (q, 4H, N-CH_2), 1.22 (t, 6H, *J*, 5.43, Hz, CH_3). ESI mass data, calc. for $[M-79]^+$, {$C_{10}H_{20}BrCdN_4S_2$} *m*/*z*: 452.9; observed *m*/*z*: 452.9.

2.2.5. Synthesis of [CdI_2(L^I-NMe-S)$_2$](**5**)

To a solution of 1-methyl-imidazolidine-2-thione (0.015 g, 0.135 mmol) in methanol (5 mL) was added a solution of cadmium(II) iodide (0.025 g, 0.068 mmol) in methanol (5 mL). The reaction mixture was stirred for 2 h at room temperature and slow evaporation at room temperature formed pale yellow crystals of **5** (70%, m.p 124–126 °C). *Anal.* Calc. for $C_8H_{16}CdI_2N_4S_2$: C, 16.05; H, 2.69; N, 9.36. Found: C, 16.08; H, 2.65; N, 9.25%. IR bands (KBr, cm^{-1}): ν(N–H) 3314 s; ν(C–H) 2917 m, 2890 m, 2793 w; ν(C–C) + ν(C–N) + δ(C–H) 1541 s, 1504 s, 1469 s, 1401 m; 1328 s, 1300 s, 1288 s, 1275 s, 1195 s; ν(C–S) 1113 s; 1022 m, 956 m, 634 s, 504 s. ^1H NMR data ($CDCl_3$ + [D_6]DMSO, δ ppm): 7.45 (s, 2H, NH), 3.69 (m, 8H, $C^{4,5}H$), 3.09 (m, 6H, CH_3). ESI mass data, calc. for $[M-127]^+$, {$C_8H_{16}CdIN_4S_2$} *m*/*z*: 472.9; observed *m*/*z*: 472.9.

2.2.6. Synthesis of [$HgCl_2$(L^I-NMe-S)$_2$] (**6**)

To a solution of 1-methyl-imidazolidine-2-thione (0.0215 g, 0.185 mmol) in methanol (5 mL) was added a solution of mercury(II) chloride (0.025 g, 0.092 mmol) in methanol (5 mL). The reaction mixture was stirred for 2 h at room temperature and a white precipitate was formed. To the precipitate was added dichloromethane (5 mL) and methanol (5 mL). Slow evaporation at room temperature formed colorless crystals of **6** (70%, m.p 140–142 °C). *Anal.* Calc. for $C_8H_{16}Cl_2HgN_4S$: C, 19.07; H, 3.20; N, 11.12. Found: C, 19.10; H, 2.96; N, 11.20%. IR bands (KBr, cm^{-1}): ν(N–H) 3219 s; ν(C–H) 2928 w, 2888 w; ν(C–C) + ν(C–N) + δ(C–H) 1556 s, 1515 s, 1472 m, 1421 w, 1407 m; 1334 w, 1310 s, 1288 s, 1195 w; ν(C–S) 1113 s; 960 m, 634 m, 583 m, 500 s. ^1H NMR data ([D_6]DMSO, δ ppm): 8.87 (s, 2H, NH), 3.86 (m, 4H, C^4H), 3.72 (m, 4H, C^5H), 3.13 (m, 6H). ESI mass data, calc. for $[M-35]^+$, [$C_8H_{16}ClHgN_4S$] *m*/*z*: 469.0; observed *m*/*z*: 469.0. Other peaks, calc. for $[HgCl(L^I\text{-NMe-S})]^+$, *m*/*z*: 353.0, observed *m*/*z*: 353.0; calc. for $[Hg(L^I\text{-NMe-S})_2\text{-H}]^+$ *m*/*z*: 433.0; observed *m*/*z*: 433.0.

2.2.7. Synthesis of [$HgCl_2$(L^{III}-NPr^n-S)$_2$] (**7**)

To a solution of 1-propyl-imidazolidine-2-thione (0.027 g, 0.184 mmol) in methanol (5 mL) was added a solution of mercury(II) chloride (0.025 g, 0.092 mmol) in methanol (5 mL). The

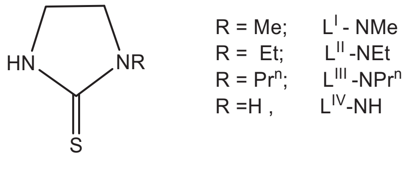

Chart 1. Heterocyclic thione ligands.

Table 1
Crystallographic data for complexes **1**–**8**.

	1	**2**	**3**	**4**
Empirical formula	$C_{10}H_{20}Cl_2N_4S_2Zn$	$C_8H_{16}I_2N_4S_2Zn$	$C_8H_{16}Br_2CdN_4S_2$	$C_{10}H_{20}Br_2CdN_4S_2$
M	396.99	550.57	504.60	532.64
T (K)	173(2)	296(2)	296(2)	173(2)
Crystal system	monoclinic	monoclinic	monoclinic	monoclinic
Space group	$P2_1/c$	$P2_1/c$	$P2_1/c$	$C1\ 2/c$
a (Å)	12.3192(4)	7.2991(6)	7.1442(3)	13.0221(10)
b (Å)	10.4013(4)	14.8870(12)	14.4504(5)	10.5580(8)
c (Å)	13.0932(4)	15.2939(12)	15.3547(5)	13.3815(8)
α (°)	90.00	90.00	90.00	90.00
β (°)	96.209(3)	93.496(3)	93.0550(10)	100.678(7)
γ (°)	90.00	90.00	90.00	90.00
V (Å^3)	1667.86(10)	1658.8(2)	1582.91(10)	1807.9(2)
Z	4	4	4	4
D_{calc} (g cm^{-3})	1.580	2.205	2.117	1.957
μ (mm^{-1})	7.270	5.441	6.677	5.852
F(000)	816	1036	968	1032
Reflections collected	11209	17341	18684	7719
Unique reflections	3160 (R_{int}, 0.0464)	4413 (R_{int}, 0.0258)	4733 (R_{int}, 0.0421)	2235 (R_{int}, 0.0307)
Data/restraints/parameters	3160/0/175	4413/2/162	4733/2/162	2235/5/97
Reflections with [$I > 2\sigma(I)$]	2885	3813	3460	1733
R indices [$I > 2\sigma(I)$]				
R_1	0.0402	0.0244	0.0413	0.0327
WR_2	0.1084	0.0586	0.0892	0.0697
R indices (all data)				
R_1	0.0435	0.0304	0.0646	0.0510
WR_2	0.1120	0.0613	0.0973	0.0772
Largest difference in peak and hole (e Å^{-3})	0.799 and −0.634	0.491 and −1.211	1.389 and −0.896	0.487 and −0.664
	5	**6**	**7**	**8**
Empirical formula	$C_8H_{16}CdI_2N_4S_2$	$C_8H_{16}Cl_2HgN_4S_2$	$C_{12}H_{24}Cl_2Hg\ N_4S_2$	$C_8H_{16}HgI_2N_4S_2$
M	598.57	503.86	559.96	686.76
T (K)	295(2)	173(2)	173(2)	173(2)
Crystal system	monoclinic	monoclinic	trigonal	monoclinic
Space group	$P2_1/c$	$P2_1/c$	R-3c	$P2_1/c$
a (Å)	7.4457(8)	13.0806(3)	20.9760(8)	7.3280(2)
b (Å)	15.0494(13)	7.99662(16)	20.9760(8)	14.9890(5)
c (Å)	15.4591(16)	14.3383(3)	22.6458(10)	15.2160(6)
α (°)	90.00	90.0	90.00	90.0
β (°)	93.362(11)	100.243(2)	90.00	93.169(3)
γ (°)	90.00	90.0	120.00	90.0
V (Å^3)	1729.3(3)	1475.90(5)	8629.1(8)	1668.76(10)
Z	4	4	18	4
D_{calc} (g cm^{-3})	2.299	2.267	1.940	2.734
μ (mm^{-1})	5.062	11.057	8.521	13.161
F(000)	1112	952	4860	1240
Reflections collected	16170	13277	9482	18457
Unique reflections	6547 (R_{int}, 0.0419)	4130 (R_{int}, 0.0300)	3238 (R_{int}, 0.0337)	5515 (R_{int}, 0.0586)
Data/restraints/parameters	6547/0/157	4130/0/165	3238/0/97	5515/2/163
Reflections with [$I > 2\sigma(I)$]	4822	3560	2608	4529
R indices [$I > 2\sigma(I)$]				
R_1	0.0604	0.0244	0.0304	0.0402
WR_2	0.1211	0.0555	0.0596	0.0928
R indices (all data)				
R_1	0.0865	0.0314	0.0459	0.0530
WR_2	0.1339	0.0577	0.0644	0.0995
Largest difference in peak and hole (e Å^{-3})	2.634 and −1.966	1.766 and −0.940	1.540 and −1.548	3.025 and −2.776

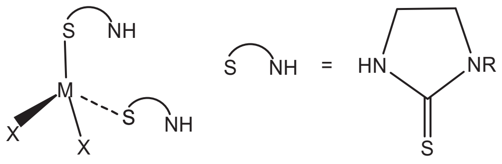

1-8

R = Me (**2, 3, 5, 6, 8**); Et (**1, 4**); Pr^n(**7**)
X = Cl(**1, 6,7**); Br(**3, 4**); I(**2, 5, 8**)
M = Zn(**1, 2**); Cd(**3, 4, 5**): Hg(**6, 7, 8**)

Scheme 1. Synthesis of complexes.

reaction mixture was stirred for 2 h at room temperature and a white precipitate was formed. To the precipitate was added dichloromethane (5 mL) and methanol (5 mL). Slow evaporation at room temperature formed colorless crystals of **7** (75%, m.p 123–125 °C). *Anal.* Calc. for $C_{12}H_{24}Cl_2HgN_4S_2$: C, 25.74; H, 4.32; N, 10.01. Found: C, 25.78; H, 4.40; N, 10.10%. IR bands (KBr, cm^{-1}): ν(N–H) 3234 s; ν(C–H) 3018 w, 2962 s, 2928 s, 2896 m, 2871 m; ν(C–C) + ν(C–N) + δ(C–H) 1542 s, 1514 s, 1479 s, 1462 m, 1443 w, 1383 w, 1360 w, 1345 m, 1317 s, 1288 s, 1252 s, 1200 m; ν(C–S) 1127 s; 1082 w, 1033 w, 981 w, 896 w, 881 m, 797 w, 650 w, 620 s, 559 s, 502 s. ^{1}H NMR data (CDCl$_3$, δ ppm): 9.07 (s, 2H, NH), 3.78 (m, 8H, C^{4,5}H), 3.48 (m, 4H, N–CH$_2$), 1.65 (m, 4H, CH$_2$), 0.92 (m, 6H, CH$_3$). ESI mass data: calc. for [M−35]$^+$, {$C_{12}H_{24}ClHgN_4S_2$} m/z: 525.1; observed m/z: 525.1. Other peaks, calc. for [HgCl(L^{III}-NPr^n-S)]$^+$, m/z: 381.0, observed m/z: 381.0; calc. for [Hg(L^{III}-NPr^n-S)$_2$-H], m/z: 489.1, observed m/z: 489.1.

Table 2
^{1}H NMR spectral data (δ in ppm) of complexes **1–8**.

	–NH	Ring protons	–N-R
L^{I}-NMe	5.7 sb	3.72 m (C^4H), 3.57 (C^5H)	3.15 s (CH_3)
LI^{I}-Net	6.02 sb	3.65 m ($C^{4,5}H$)	3.65 m (N-CH_2), 1.21 m (CH_3)
L^{III}-NPr^n	5.90 sb	3.65 m (C^4H), 3.49 t (C^5H)	3.65 m (N-CH_2), 1.65 (*CH_2*), 0.97 m (CH_3)
1[a]	8.42 sb	3.72 m ($C^{4,5}H$)	3.57 m (N-CH_2), 1.20 m (CH_3)
2[b]	7.04 sb	3.73 m ($C^{4,5}H$)	3.14 m (CH_3)
3[b]	7.75 sb	3.67 m ($C^{4,5}H$)	3.07 m (CH_3)
4[a]	7.95 sb	3.76 m ($C^{4,5}H$)	3.61 q (N-CH_2), 1.22 t (CH_3)
5[b]	7.45 sb	3.69 m ($C^{4,5}H$)	3.09 m (CH_3)
6[c]	8.87 sb	3.86 m (C^4H), 3.72 m (C^5H)	3.13 m (CH_3)
7[a,d]	9.07 sb	3.78 m ($C^{4,5}H$)	3.48 m (N-CH_2), 1.65 (CH_2), 0.92 (CH_3)
8[a]	7.14 sb	3.80 m ($C^{4,5}H$)	3.14 s (CH_3)

[a] $CDCl_3$.
[b] ($CDCl_3$ + D_6[DMSO]).
[c] D_6[DMSO].
[d] N-Pr^n = N-$CH_2CH_2CH_3$.

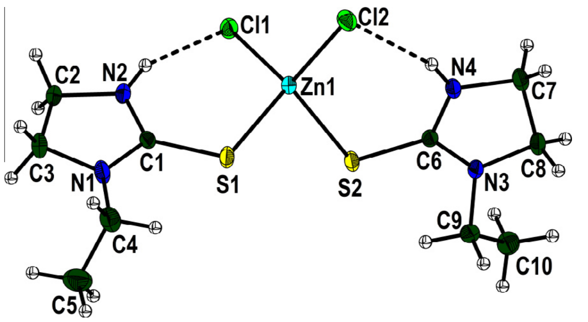

Fig. 1. ORTEP showing the molecular structure of [$ZnCl_2(L^{II}$-NEt$)_2$] (**1**) and the intra molecular H-bonding, S···S distance (3.563 Å) (with 30% probability).

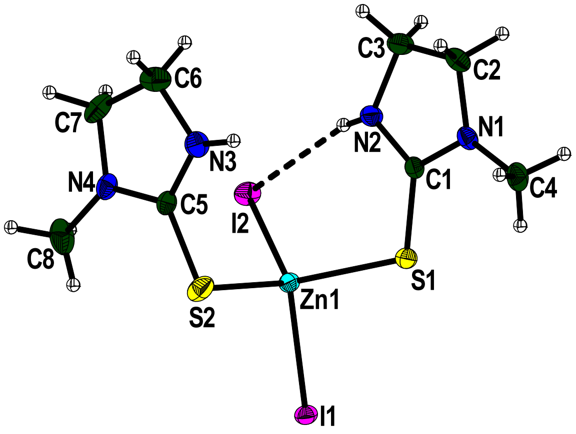

Fig. 2. ORTEP showing the molecular structure of [$ZnI_2(L^{I}$-NMe$)_2$] (**2**) and intra molecular H bonding, S···S distance (3.924 Å) (with 30% probability).

2.2.8. Synthesis of [$HgI_2(L^{I}$-NMe-S$)_2$] (**8**)

To a solution of 1-methyl-imidazolidine-2-thione (0.013 g, 0.112 mmol) in methanol (5 mL) was added a solution of mercury(II) iodide (0.025 g, 0.055 mmol) in methanol (5 mL). The reaction mixture was stirred for 2 h at room temperature. To this mixture was added dichloromethane (5 mL) and slow evaporation at room temperature formed pale yellow crystals of **8** (71%, m.p 103–105 °C). *Anal.* Calc. for $C_8H_{14}HgI_2N_4S_2$: C, 14.03; H, 2.06; N, 8.18. Found: C, 13.85; H, 2.20; N, 8.10%. IR bands (KBr, cm^{-1}): ν(N–H) 3313 s; ν(C–H) 2917 m, 2887 m, 2792 w; ν(C–C) + ν(C–N) + δ(C–H) 1540 s, 1504 s, 1468 s, 1401 m; 1328 s, 1298 s, 1286 s, 1194 s; ν(C–S) 1111 s; 1022 m, 954 m, 633 s, 504 s. ^{1}H NMR data ($CDCl_3$, δ ppm): 7.14 (s, 2H, NH), 3.80 (m, 8H, $C^{4,5}H$), 3.14 (s, 6H, CH_3).

2.3. X-ray crystallography

The single crystals of the compounds were mounted on glass fibers and data were collected using Xcalibur, Eos, Gemini (**1**, **4**, **6**, **7** and **8**), Xcalibur, Ruby, Gemini (**5**) and Bruker APEX-II CCD (**2** and **3**) diffractometers, equipped with a graphite monochromator and Mo Kα (λ = 0.71073 Å; **2–8**,) and Cu Kα radiation (λ = 1.54184 Å; **1**). The unit cell dimensions and intensity data were measured at 173(2) K for **1**, **4**, **6**, **7** and **8**, 295(2) K for **5** and at 296(2) K for **2** and **3**. The data were processed with CRYSALISPRO (data collection, cell refinement) (**1**, **4–8**), CRYSALISRED (data reduction) (**1**, **4**, **6** and **8**), CRYSALISPRO (data reduction) (**5** and **7**) [45], Bruker APEX2 (data collection) and Bruker SAINT (cell refinement, data reduction) (**2** and **3**) [46]. The structures were solved by direct methods using the programs SHELXS97 [47] (**1**, **4–8**) and SIR-92 (**2** and **3**) [48], and refined by full-matrix least-squares techniques against F^2 using SHELXL-97 [49]. The crystallographic data are given in Table 1, while detailed bond lengths/angles are available in the Supplementary material. The asymmetric unit of compound **4** contains one half-molecule situated on a twofold rotational axis centered on the cadmium atom. Disorder is modeled for both

Table 3
Important bond lengths (Å) and angles (°) of complexes **1–8**.

M	X	N–R	M–X	M–S	C–S	S–M–S (X–M–X)	M–S–C
Zn (**1**)	Cl	Et	2.2517(7), 2.2531(7)	2.3703(7), 2.3657(7)	1.715(3), 1.713(3)	97.58(3) [110.60(3)]	110.44(9), 109.84(9)
Zn (**2**)	I	Me	2.5962(4), 2.5964(4)	2.3495(8), 2.3653(8)	1.699(3), 1.717(3)	112.63(4) [113.432(13)]	108.72(9), 96.65(9)
Cd (**3**)	Br	Me	2.5695(5), 2.5780(5)	2.5438(12), 2.5224(12)	1.716(4), 1.701(4)	114.23(5) [116.036(19)]	106.29(13), 94.18(13)
Cd (**4**)	Br	Et	2.5499(5)	2.5464(11)	1.694(3)	103.47(7) [111.74(3)]	110.22(13)
Cd (**5**)	I	Me	2.7494(6), 2.7511(6)	2.5409(17), 2.5538(18)	1.697(6), 1.714(7)	111.61(7) [114.99(2)]	107.40(19), 94.7(2)
Hg (**6**)	Cl	Me	2.5372(8), 2.5161(7)	2.4782(8), 2.4985(9)	1.719(3), 1.718(3)	119.18(3) [102.43(3)]	105.96(12), 105.98(11)
Hg (**7**)	Cl	Pr^n	2.5105(8), 2.5104(8)	2.5001(8), 2.5001(8)	1.715(3)	112.32(4) [107.26(4)]	106.21(11)
Hg (**8**)	I	Me	2.7466(4), 2.7634(3)	2.5376(14), 2.5655(16)	1.701(5), 1.711(6)	110.68(6) [114.306(13)]	105.89(18)

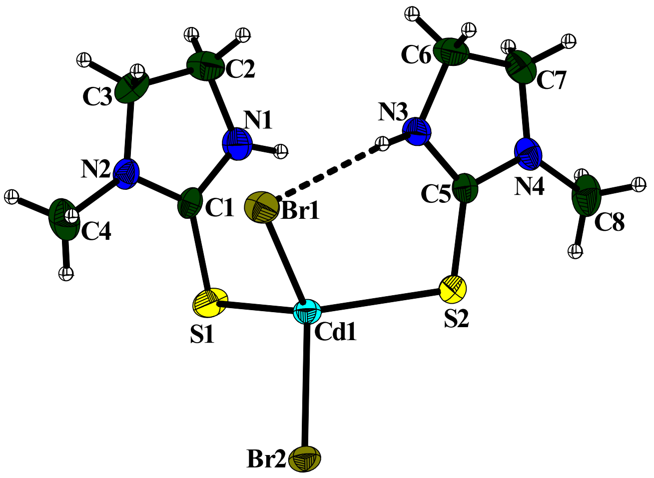

Fig. 3. ORTEP showing the molecular structure of $[CdBr_2(L^{I}\text{-NMe})_2]$ (**3**) and intra molecular H-bonding, S···S distance (4.254 Å) (with 50% probability).

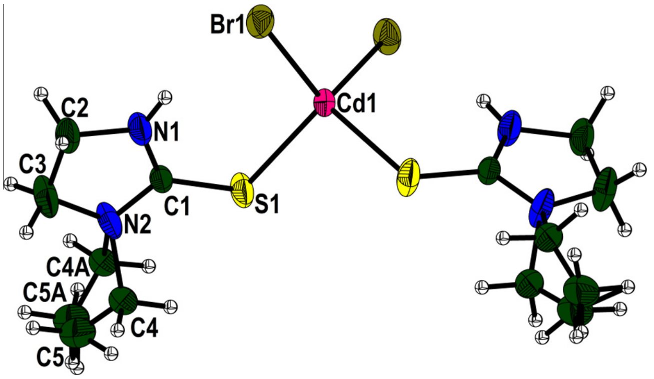

Fig. 4. ORTEP showing the molecular structure of $[CdBr_2(L^{II}\text{-NEt})_2]$ (**4**), S···S distance (3.998 Å) (with 30% probability).

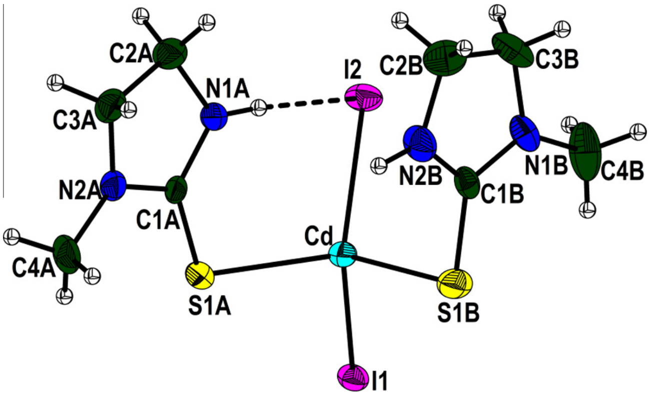

Fig. 5. ORTEP diagram showing the molecular structure of $[CdI_2(L^{I}\text{-NMe})_2]$ (**5**) (with 30% probability).

carbon atoms of the ethyl group over two sites with an occupancy ratio of 0.544(6):0.456(6). No classical hydrogen bonds are observed. Complexes **2** and **3** are isostructural.

3. Results and discussion

3.1. Comments on the synthesis

Scheme 1 shows the formation of complexes of Zn^{II}, Cd^{II} and Hg^{II} with the stoichiometry $[MX_2(L\text{-}NR)_2]$ ($L\text{-}NR = L^{I}\text{-NMe}$, $L^{II}\text{-NEt}$ and $L^{III}\text{-NPr}^{n}$, **1**–**8**). On addition of a metal salt to a solution of the thio ligand in methanol, followed by stirring, there was either formation of a white precipitate (**2**, **3**, **6** and **7**) or no precipitation (**1**, **4**, **5** and **8**). To the reaction mixture dichloromethane was added and the clear solution obtained was allowed to crystallize at room

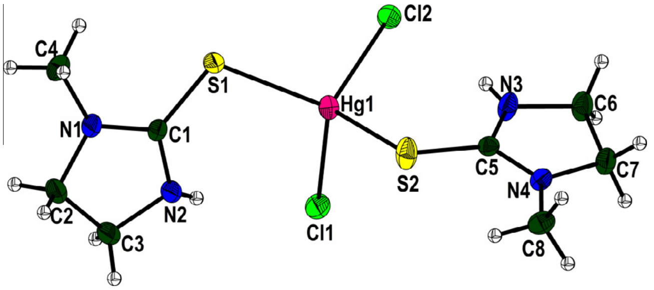

Fig. 6. ORTEP showing the molecular structure of $[HgCl_2(L^{I}\text{-NMe})_2]$ (**6**) (with 50% probability).

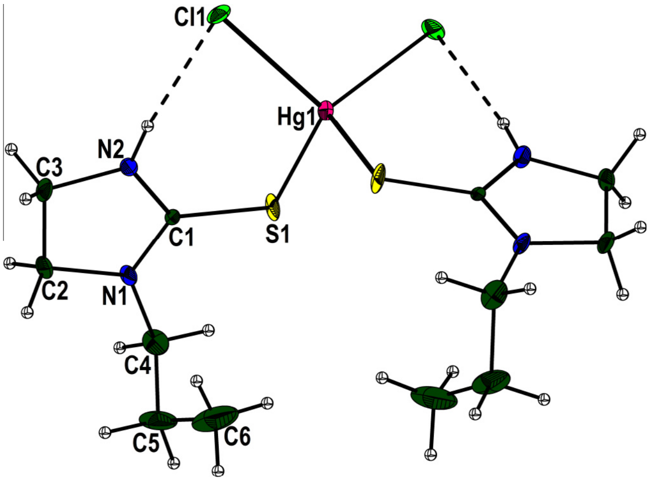

Fig. 7. ORTEP showing the molecular structure of $[HgCl_2(L^{III}\text{-NPr}^{n})_2]$ (**7**) and intra molecular H-bonding, (with 50% probability).

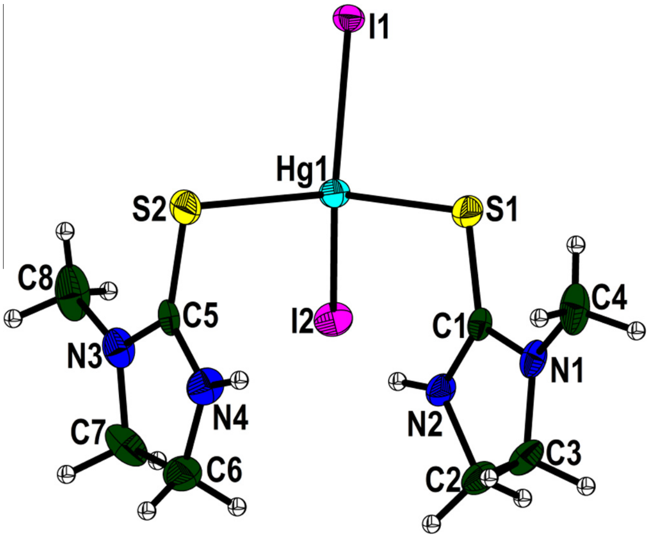

Fig. 8. ORTEP showing the molecular structure of $[HgI_2(L^{I}\text{-NMe})_2]$ (**8**) (with 50% probability).

Table 4
N–H· · ·X distances (Å) and angles (°) for complexes **1**–**8**.

Complex No.	d(H· · ·X)	d(N· · ·X)	∠(N–H· · ·X)
1. Cl	2.394, 2.365	3.196, 3.195	155.38, 162.31
2. I	2.856	3.643	152.97
3. Br	2.678	3.483	167.64
4. Br	2.512	3.355	163.46
5. I	2.909	3.711	156.05
6. Cl	2.644, 2.585	3.259, 3.254	167.07, 169.69
7. Cl	2.389	3.262	170.66
8. I	2.875	3.676	152.00

Note: [a]The ortep diagrams of complexes **1**, **2**, **3**, **5** and **7** depict N–H· · ·X distances (Figs. 1–5), while ortep diagrams of **4**, **6** and **8** do not show such distances and they are calculated from their diagrams prepared using the mercury program (see Supplementary data).

temperature. In this way, eight compounds were prepared which formed crystals and their molecular structures were determined using X-ray crystallography.

3.2. Spectroscopy

The IR spectra of the complexes were different from those of the ligands. For example, in complex **1**, the ν(N–H) band appeared at $3244\ \mathrm{cm^{-1}}$, which is in a higher energy region relative to the uncoordinated ligand ($\mathrm{L^{II}}$-NEt, $3188\ \mathrm{cm^{-1}}$). Other complexes showed ν(N–H) bands in the region $3219–3313\ \mathrm{cm^{-1}}$. The characteristic ν(C–S) band in complex **1** appears at $1127\ \mathrm{cm^{-1}}$, which is in a lower energy region relative to the free thio ligand ($1199\ \mathrm{cm^{-1}}$). Other complexes showed ν(C–S) bands in the region $1111–1127\ \mathrm{cm^{-1}}$ (see Section 2). The proton NMR spectra of the complexes clearly showed that the NH protons are most sensitive to coordination (Table 2). For example, the free ligand $\mathrm{L^{I}}$-NMe shows the NH proton signal at $\delta = 5.70$ ppm, and this is shifted to the low field region 7.04–8.87 ppm in its complexes **2**, **3**, **5**, **6** and **8**. Similarly, the NH proton signals of $\mathrm{L^{II}}$-NEt and $\mathrm{L^{III}}$-NPr^n at 6.02 and 5.90 ppm respectively are shifted to the low energy region 7.95–9.07 ppm in complexes **1**, **4** and **7**. The N–R protons are not much affected and only

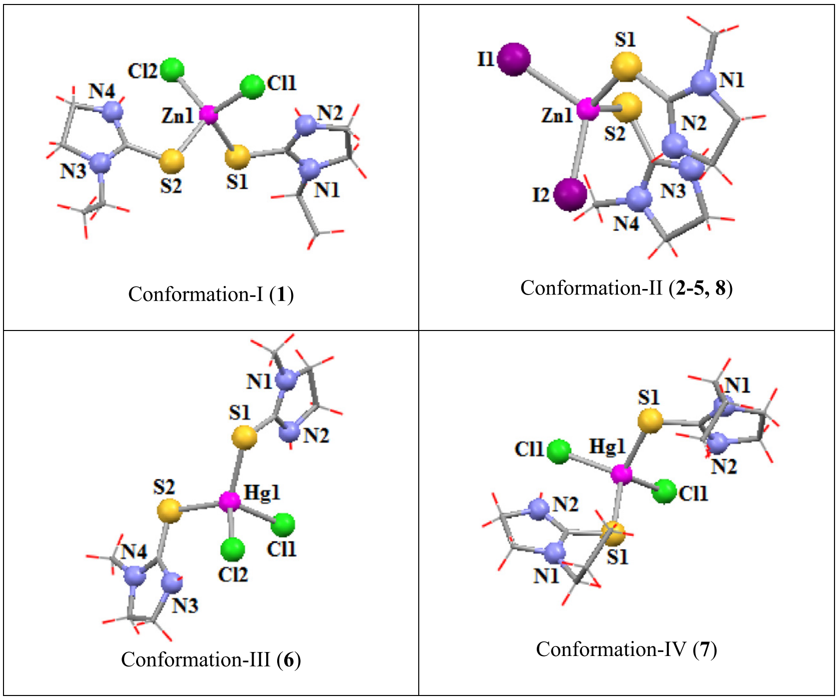

Conformation-I (**1**)
Conformation-II (**2-5, 8**)
Conformation-III (**6**)
Conformation-IV (**7**)

Fig. 9. Conformations of complexes **1**–**8**.

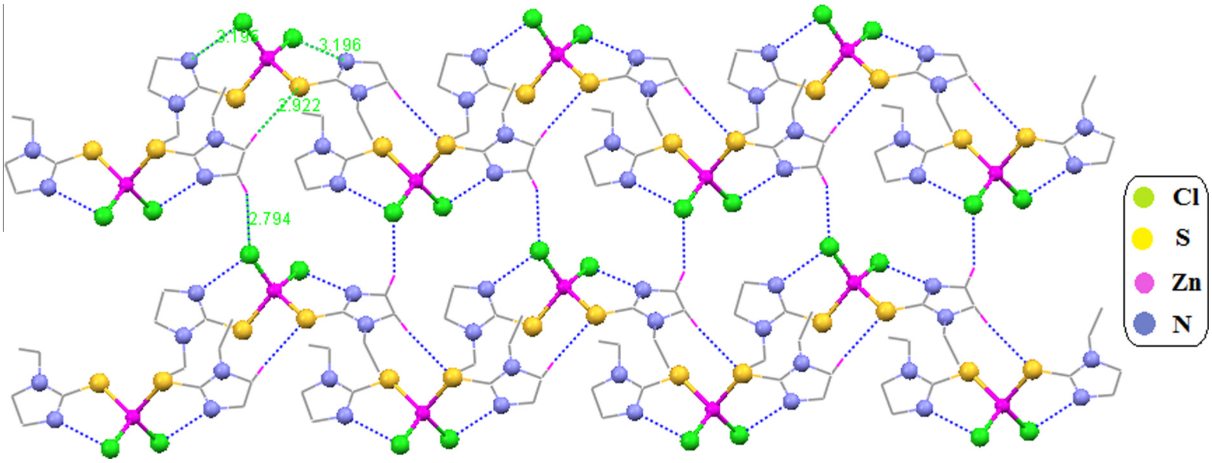

Fig. 10. H-bonded 2D polymeric network of $[\mathrm{ZnCl_2(L^{II}\text{-}NEt)_2}]$ (**1**).

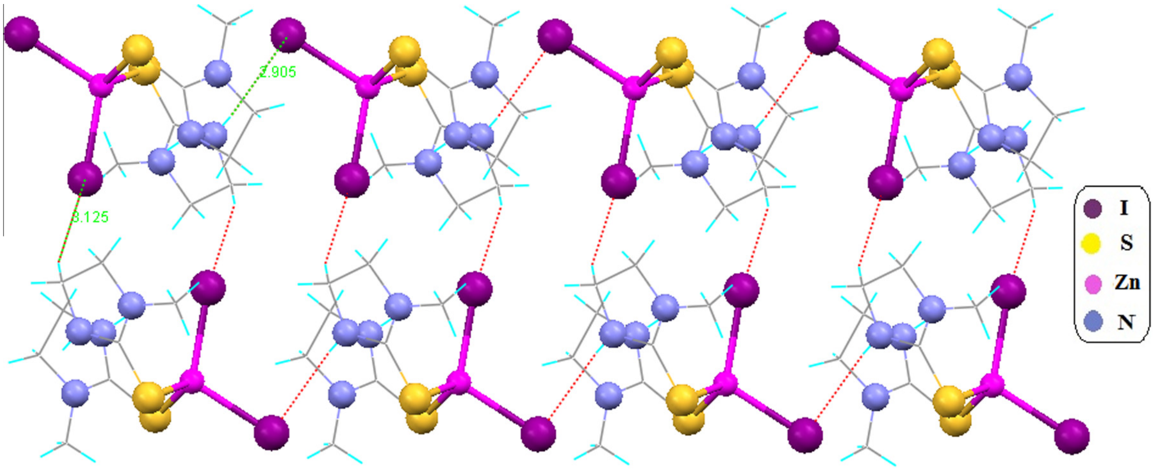

Fig. 11. H-bonded 2D polymeric network of $[ZnI_2(L^I\text{-NMe})_2]$ (**2**).

small changes occurred for the N–Me and N–CH_2 protons. The ring protons appeared as multiplets and are marginally affected in complexes **1**–**8**.

3.3. Molecular structures

The crystal data of complexes **1**–**8** are given in Table 1. Complexes **1**–**6** and **8** crystallized in the monoclinic system with each having space group $P2_1/c$, except for complex **4** with the space group $C2/c$, and complex **7** crystallized in the trigonal system with the space group $R\text{-}3c$. In the complex $[ZnCl_2(L^{II}\text{-NEt-S})_2]$ (**1**) (Fig. 1), Zn^{II} is bonded to two chlorine atoms at Zn–Cl distances of 2.2517(7) and 2.2531(7) Å, and to two S atoms at Zn–S distances of 2.3703(7) and 2.3657(7) Å (Table 3). These distances are similar to those observed in the literature [37]. The S–Zn–S and Cl–Zn–Cl angles of 97.58(3) and 110.60(3)° respectively are less than those {S–Zn–S, 110.71(2)°; Cl–Zn–Cl, 114.59(2)°} observed in the analogous complex $[ZnCl_2(L^I\text{-NMe-}S)_2]$ [37]. The difference is attributed to the effect of the substituents at one nitrogen atom of the thio ligand. The bonding pattern of the complex $[ZnI_2(L^I\text{-NMe-S})_2]$ (**2**) (Fig. 2) is similar to that of complex **1**. While the Zn–S distances are similar, the S–Zn–S angle of 112.65(4)° is larger, as compared to that of complex **1**. The difference is attributed to the closer S···S distance (3.563 Å) in complex **1** vis-à-vis that in complex **2** (3.924 Å). The Zn–S, Zn–Cl and Zn–I distances {Zn–I, 2.5961(4), 2.5964(4) Å} are less than the corresponding sum of the ionic radii {Zn^{2+} and S^{2-}, 2.58; Zn^{2+} and Cl^-, 2.55; Zn^{2+} and I^-, 2.94 Å} [50]. The molecular structures of complexes **3**–**8** (Figs. 3–8) are similar to that of complex **1**. The Cd–S distances (complexes **3**–**5**) lie in the range 2.5224(12)–2.5538(18) Å, which are comparable to the literature trends [36]. Similarly, the Hg–S distances (complexes **6**–**8**) lie in the range 2.4782(8)–2.5660(16) Å, which are comparable to the

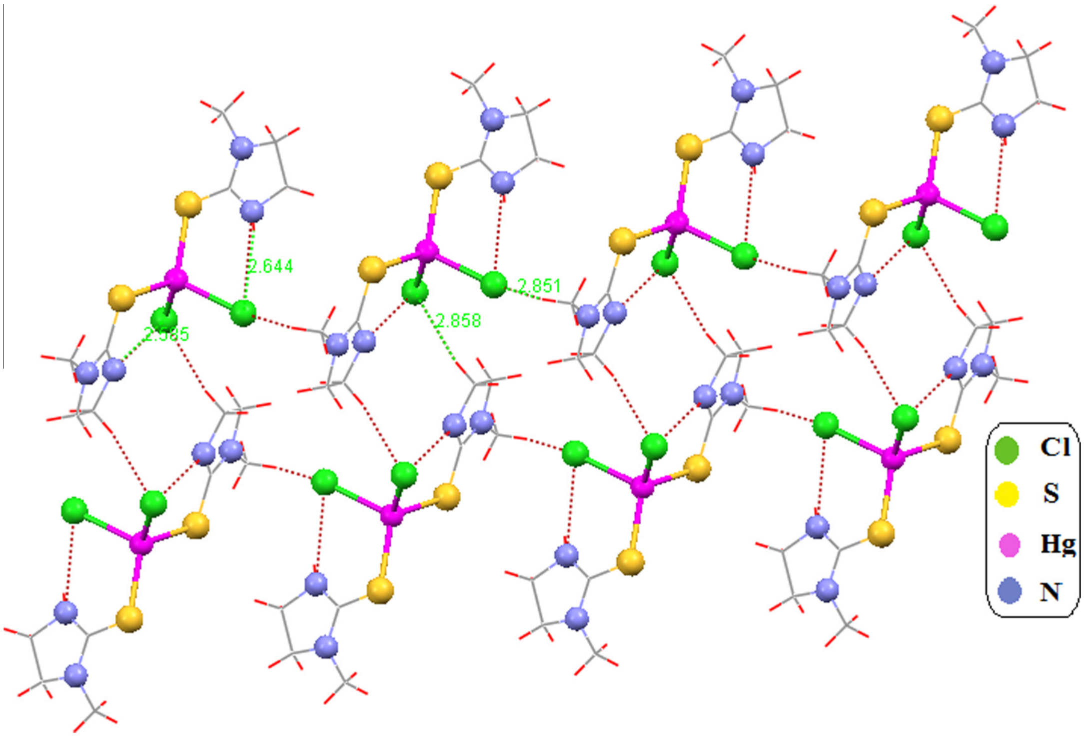

Fig. 12. H-bonded 2D polymeric network of $[HgCl_2(L^I\text{-NMe})_2]$ (**6**).

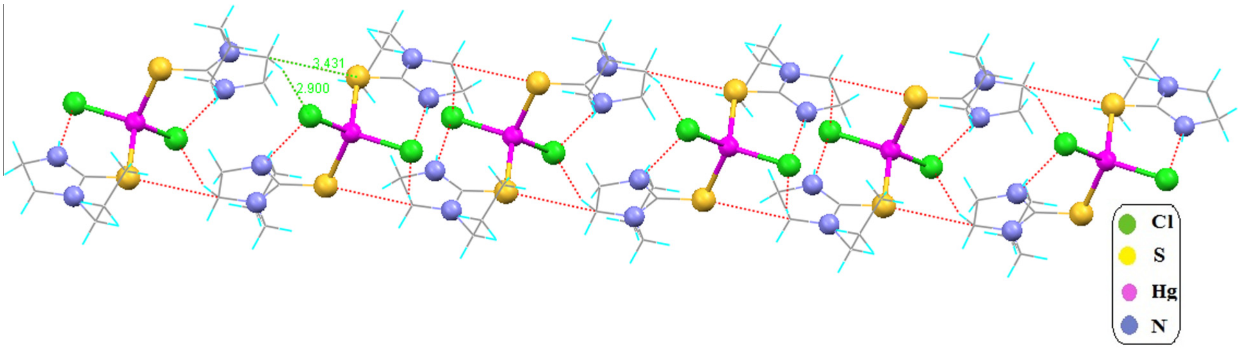

Fig. 13. H-bonded 1D polymeric network of [HgCl$_2$(L^{III}-NPr^n)$_2$] (**7**).

$[M]^+ \rightarrow [M\text{-}X]^+$ (**1-7**)$\rightarrow [M\text{-}X\text{-}L]^+$ (**6**,**7**) $\rightarrow [M\text{-}H\text{-}X_2]^+$ (**6**,**7**)

Scheme 2. Fragmentation steps, [M]$^+$ = molecular ion.

literature trends [36,40]. In the Cd/Hg complexes, the S–M–S and X–M–S angles lie in the wide range 103.45(7)–119.18(3)°. In complex **1**, the C–S bond distance of 1.715(3) Å lies between C–S single (1.81 Å) and C–S double (1.62 Å) bond distance values, indicating partial double bond character [51] and the weakening of the bond is due to the coordination of the ligand to Zn^{II}. Similar behavior is observed in complexes **2**–**8**, and here the C–S bond distances fall in the wide range 1.696(3)–1.721(4) Å. It is noted that the C–S distances do not vary in a systematic manner, either with respect to the halogen or the metal atom.

3.4. Intra- and intermolecular interactions

In complexes **1**–**8**, there is intra molecular N–H···X (X = Cl, Br, I) hydrogen bonding. The N–H···X, N···X distances and N–H···X angles are given in Table 4. The N···Cl, N···Br and N···I distances lie in the ranges 3.195–3.262, 3.483–3.355 and 3.643–3.711 Å respectively. These distances are either less than or close to the sum of the van der Waals radii of N and X {nitrogen and chlorine = 3.25–3.45 Å, nitrogen and bromine = 3.35–3.55 Å and nitrogen and iodine = 3.50–3.67 Å} [50].

Fig. 9 shows the conformations adopted by the complex molecules. Interestingly there are four types of conformations: conformation I (**1**), conformation II (**2**–**5**, **8**), conformation III (**6**), and conformation IV (**7**). Each of complexes **1**, **6** and **7** have different intermolecular interactions, while complexes **2**–**5** and **8** have the same type of intermolecular interactions. These conformations give rise to four types of intermolecular interactions which result in the formation of 2D (**1**–**6**, **8**) or 1D (**7**) polymeric networks. These networks are delineated in Figs. 10–13.

In the case of complex **1**, the sulfur atom of the imidazole ring of one molecule interacts with the CH hydrogen atom of imidazole ring of second molecule through C–H···S, and C···S interactions {C–H···S, 2.922 Å, C···S 3.875 Å; C–H···S angle 166.93°} resulting in the formation of a 1D chain. The C···S distance is greater than the sum of the van der Waals radii of carbon and sulfur, 3.45–3.50 Å [50]. The C–H hydrogen atom of the imidazole ring in one linear chain forms a H-bond with the chlorine atom {C–H···Cl, 2.794 Å; C–H···Cl, 154.54°}, of a second chain, resulting in the formation of a 2D polymer (Fig. 10).

In complex **2**, the intermolecular interaction between the imino hydrogen and iodine atom of a second molecule {NH···I, 2.905 Å; N–H···I angle, 162.43°} leads to the formation of a 1D polymeric chain. These chains further interact with each other through C–H···I interactions between the CH hydrogen atom of the imidazole ring and an iodine atom of a second chain {C–H···I, 3.125 Å; C–H···I angle, 155.16°}, resulting in the formation of a 2D network (Fig. 11). The interactions in complexes **3** and **5** and are similar (see Supplementary data). In complex **6**, the intermolecular hydrogen bonding interaction between the N–CH$_3$ hydrogen of the imidazole ring and the chlorine atom of a second molecule {CH···Cl, 2.851 Å; C–H···Cl angle, 126.68°} leads to the formation of a 1D polymeric

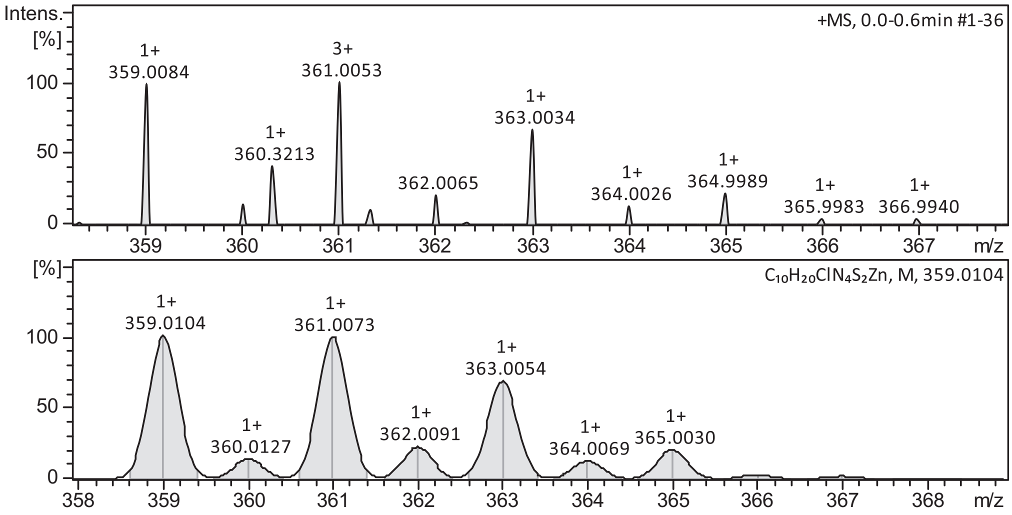

Fig. 14. Observed peak m/z = 359.0 and its isotropic pattern m/z 359.0, [M−Cl]$^+$, C$_{10}$H$_{20}$ClN$_4$S$_2$Zn (**1**).

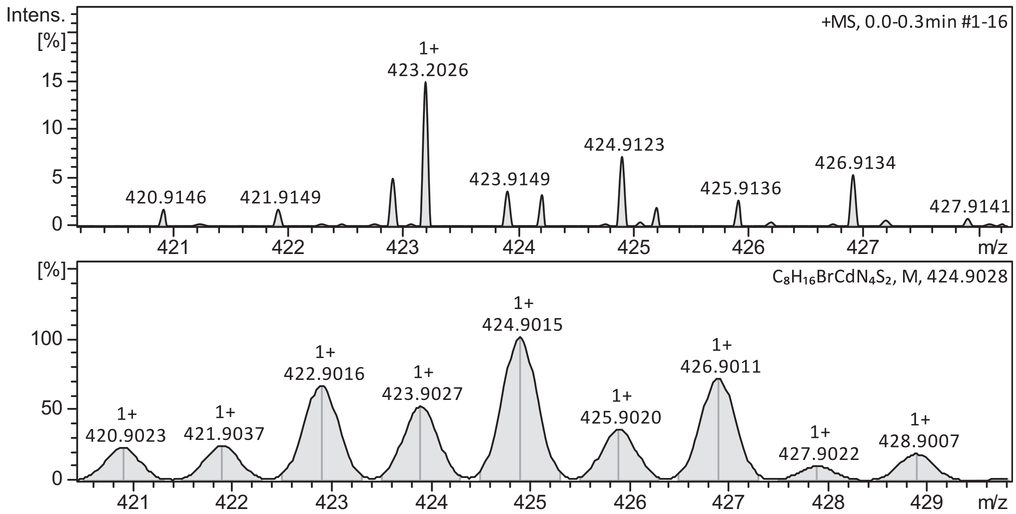

Fig. 15. Observed peak $m/z = 423.20$ and its isotropic pattern m/z 424.9, $[M{-}Br]^+$, $C_8H_{16}BrN_4S_2Cd$ (**3**).

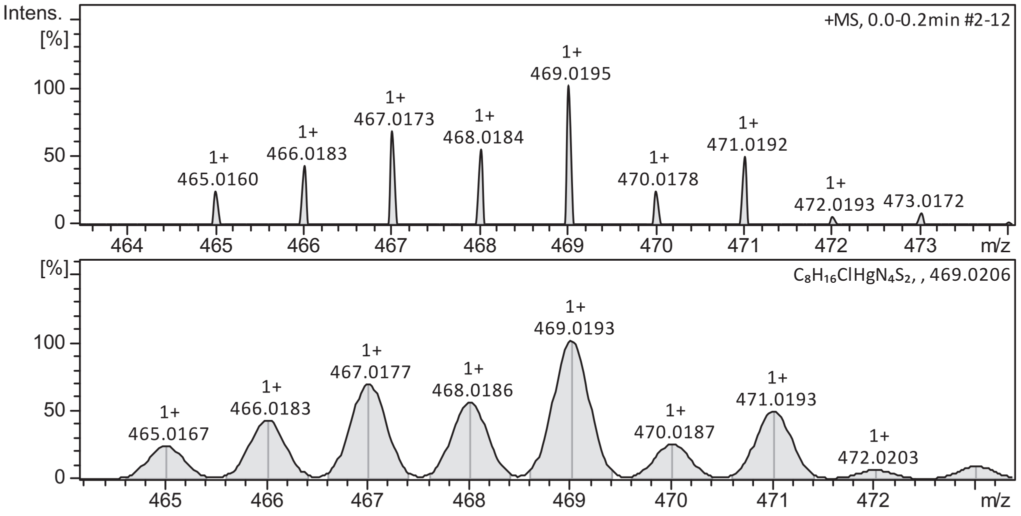

Fig. 16. Observed peak $m/z = 469.0$ and its isotropic pattern m/z 469.0, $[M{-}Cl]^+$, $C_8H_{16}ClN_4S_2Hg$ (**6**).

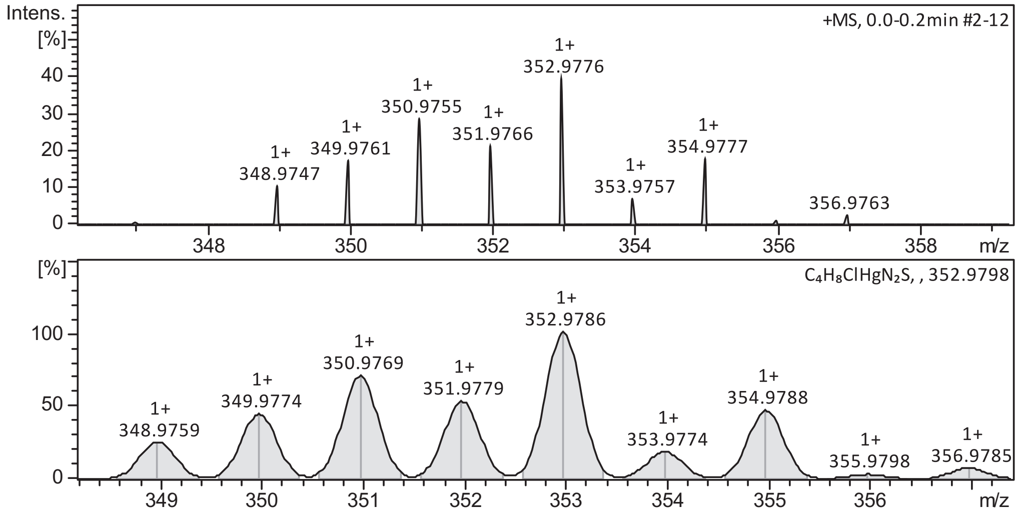

Fig. 17. Observed peak $m/z = 353.0$ and its isotropic pattern m/z 353.0, $[M{-}Cl{-}(L^{I}\text{-}NMe)]^+$ $C_4H_8ClN_2SHg$ (**6**).

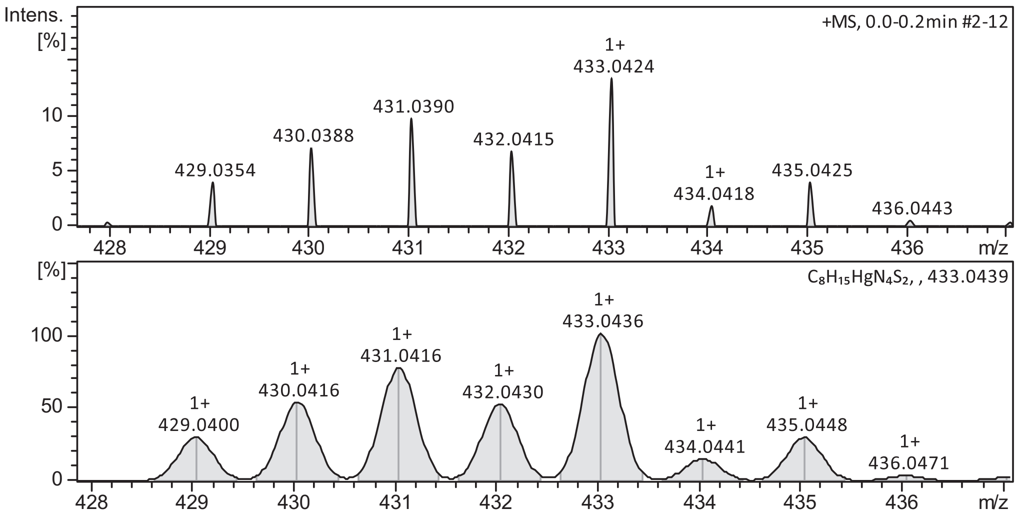

Fig. 18. Observed peak *m*/*z* = 433.0 and its isotropic pattern *m*/*z* 433.0, $[M{-}H{-}Cl_2]^+$, $C_8H_{15}N_4S_2Hg$ (**6**).

chain. These chains further interact with each other through C–H···Cl interactions between the CH hydrogen atom of the imidazole ring and the chlorine atom of a second chain {C–H···Cl, 2.858 Å; C–H···Cl angle, 140.24°}, resulting in the formation of a 2D network (Fig. 12). The packing diagram of complex **7** shows that the sulfur atom of the imidazole ring in one molecule interacts with the C atom of imidazole ring of a second molecule through {C···S 3.431 Å} interactions and the CH hydrogen atom of a ligand in one linear chain forms an H-bond with the chlorine atom {C–H···Cl, 2.900 Å; C–H···Cl, 165.33°} of a second molecule, resulting in the formation of a 1D polymeric chain (Fig. 13). The C···S distance is marginally less than the sum of the van der Waals radii of carbon and sulfur, 3.45–3.50 Å [50].

3.5. ESI-mass

An ESI mass spectral study of the complexes did not shown the molecular ion, $[M]^+$, but all the complexes (**1**–**7**) on which this study was carried out have shown prominent peaks corresponding to $[M{-}X]^+$ ions (here X represents a halogen). Complexes **6** and **7** showed additional peaks corresponding to $[M{-}X{-}L]^+$ (L is the neutral thio ligand) and $[M{-}H{-}X_2]^+$ species. Scheme 2 shows the formation of the various species. Representative ESI-mass signals are shown in Figs. 14–18.

4. Conclusion

Substituted imidazolidine-2-thiones with divalent metal ions, Zn–Hg, have formed distorted tetrahedral complexes. The complex molecules adopt four types of conformations which give rise to different patterns of intermolecular interactions and hence 2D (**1**–**6**, **8**) or 1D (**7**) polymeric networks are obtained. ESI-mass has shown that a halogen is easily lost and thus complexes **1**–**7** displayed molecular ions with the loss of one halogen in each case, viz., $[M{-}X]^+$ ions. This reveals that the M–S bonds are quite strong and the thio ligands remain bonded to the metal ions. In complexes **6** and **7**, further loss of both halogens gave $[M{-}(L_2\text{-}H)]^+$ ions. In addition, these two complexes also formed, $[M{-}X{-}L]^+$ ions by losing one halogen and one thio ligand from their respective molecular ions.

Acknowledgments

Financial assistance from UGC (BSR), New Delhi – India and the Council of Scientific and Industrial Research (CSIR), New Delhi – India, Emeritus Grant [21(0904)/12-EMR-II] to T.S. Lobana, New Delhi are gratefully acknowledged.

Appendix A. Supplementary data

CCDC 1007794–1007801 contain the supplementary crystallographic data for complexes **1**–**8**. These data can be obtained free of charge via http://www.ccdc.cam.ac.uk/conts/retrieving.html, or from the Cambridge Crystallographic Data Centre, 12 Union Road, Cambridge CB2 1EZ, UK; fax: (+44) 1223-336-033; or e-mail: deposit@ccdc.cam.ac.uk. Supplementary data associated with this article can be found, in the online version, at http://dx.doi.org/10.1016/j.poly.2014.10.016.

References

[1] E.S. Raper, Coord. Chem. Rev. 153 (1996) 199.
[2] E.S. Raper, Coord. Chem. Rev. 129 (1994) 91.
[3] E.S. Raper, Coord. Chem. Rev. 165 (1997) 475.
[4] J.A. Garcia-Vazquez, J. Romero, A. Sousa, Coord. Chem. Rev. 193 (1999) 691.
[5] P.D. Akrivos, Coord. Chem. Rev. 213 (2001) 181.
[6] A. Kaltzoglou, P.J. Cox, P. Aslanidis, Inorg. Chim. Acta 358 (2005) 3048.
[7] A.J. Blake, V. Lippolis, T. Pivetta, G. Verani, Acta Crystallogr., Sect. C: Cryst. Struct. Commun. 63 (2007) m364.
[8] T.S. Lobana, R. Sharma, G. Hundal, R.J. Butcher, Inorg. Chem. 45 (2006) 9402.
[9] T.S. Lobana, R. Sharma, R. Sharma, S. Mehra, A. Castineiras, P. Turner, Inorg. Chem. 44 (2005) 1914.
[10] T.S. Lobana, R. Sharma, R.J. Butcher, Polyhedron 27 (2008) 1375.
[11] R. Sultana, T.S. Lobana, R. Sharma, A. Castineiras, T. Akitsu, K. Yahagi, Y. Aritake, Inorg. Chim. Acta 363 (2010) 3432.
[12] T.S. Lobana, R. Sultana, R.J. Butcher, J.P. Jasinski, J.A. Golen, A. Castineiras, K. Propper, F.J. Fernandez, M. Cristina Vega, J. Organomet. Chem. 745–746 (2013) 460.
[13] T.S. Lobana, R. Sultana, R.J. Butcher, J.P. Jasinski, T. Akitsu, Z. Anorg. Allg. Chem. 640 (2014) 1688.
[14] T.S. Lobana, R. Sultana, A. Castineiras, R.J. Butcher, Inorg. Chim. Acta 362 (2009) 5265.
[15] T.S. Lobana, R. Sultana, G. Hundal, R.J. Butcher, Dalton Trans. 39 (2010) 7870.
[16] T.S. Lobana, R. Sultana, R.J. Butcher, A. Castineiras, T. Akitsu, F.J. Fernandez, M.C. Vega, Eur. J. Inorg. Chem. (2013) 5161.
[17] F. Noreen, T. Ruffer, H. Lang, A.A. Isab, S. Ahmad, J. Chem. Cryst. 38 (2008) 765.
[18] Q. Zhu, W. Chu, R. Huang, J. Zhang, Y. Xu, J. Coord. Chem. 61 (2008) 3390.
[19] G.A. Bowmaker, J.V. Hanna, C. Pakawatchai, B.W. Skelton, Y. Thanyasirikul, A.H. White, Inorg. Chem. 48 (2009) 350.
[20] E.S. Raper, J.R. Creighton, J.D. Wilson, W. Clegg, A. Milne, Inorg. Chim. Acta 155 (1989) 85.
[21] G.A. Bowmaker, J.V. Hanna, B.W. Skelton, A.H. White, Chem. Commun. (2009) 2168.
[22] D. Jia, Y. Zhang, J. Deng, M. Ji, J. Coord. Chem. 60 (2007) 833.
[23] C. Palivan, T. Berclaz, M. Geoffroy, S. Ramaprabhu, G. Bernardinelli, J. Chem. Soc., Faraday Trans. 91 (1995) 2155.
[24] L.P. Battaglia, A.B. Corradi, F.A. Devillanova, G. Verani, Transition Met. Chem. 4 (1979) 264.

[25] S. Ramaprabhu, E.A.C. Lucken, G. Bernardinelli, J. Chem. Soc., Dalton Trans. (1995) 115.
[26] S. Ramaprabhu, E.A.C. Lucken, G. Bernardinelli, J. Chem. Soc., Dalton Trans. (1993) 1185.
[27] M.S. Hussain, A.R. Al-Arfaj, M.L. Hossain, Transition Met. Chem. 15 (1990) 264.
[28] S. Friedrichs, P.G. Jones, Acta Crystallogr., Sect. C: Cryst. Struct. Commun. 55 (1999) 1625.
[29] S. Friedrichs, P.G. Jones, Z. Naturforsch., B: Chem. Sci. 59 (2004) 49.
[30] S. Friedrichs, P.G. Jones, Z. Naturforsch., B: Chem. Sci. 59 (2004) 1429.
[31] S. Friedrichs, P.G. Jones, Z. Naturforsch., B: Chem. Sci. 59 (2004) 793.
[32] S. Friedrichs, P.G. Jones, Z. Naturforsch., B: Chem. Sci. 61 (2006) 1391.
[33] P.G. Jones, S. Friedrichs, Acta Crystallogr., Sect. C: Cryst. Struct. Commun. 62 (2006) m623.
[34] A.R. Al-Arfaj, J.H. Reibenspies, A.A. Islab, M.S. Hussain, Acta Crystallogr., Sect. C 54 (1998) 51.
[35] L. Cavalca, P. Domiano, A. Musatti, P. Sgarabotto, J. Chem. Soc., Chem. Commun. (1968) 1136.
[36] M.I.M. Wazeer, A.A. Isab, M. Fettouhi, Polyhedron 26 (2007) 1725.
[37] M. Fettouhi, M.I.M. Wazeer, A.A. Isab, J. Coord. Chem. 60 (2007) 369.
[38] M. Fettouhi, M.I.M. Wazeer, A.A. Isab, Z. Kristallogr. New Cryst. Struct. 221 (2006) 221.
[39] C. Nardelli, Gazz. Chim. Ital. 88 (1958) 248.
[40] M. Cannas, F.A. Devillanova, G. Marongiu, G. Verani, J. Inorg. Nucl. Chem. 43 (1981) 2383.
[41] L. Cavalca, M. Nardelli, G. Fava, Acta Crystallogr. 13 (1960) 125.
[42] P.F. Rodesiler, N.G. Charles, E.A.H. Griffth, E.L. Amma, Acta Crystallogr., Sect. C: Cyst. Struct. Commun. 43 (1987) 1058.
[43] T.S. Lobana, R. Sharma, R. Sharma, R. Sultana, R.J. Butcher, Z. Anorg. Allg. Chem. 634 (2008) 718.
[44] J.A. Garcia-Vazquez, A. Sousa-Pedrares, M. Carabel, J. Romero, A. Sousa, Polyhedron 24 (2005) 2043.
[45] Oxford Diffraction. CrysAlisPro CCD and CrysAlisPro RED Oxford Diffraction Ltd., Yarnton, England, 2009.
[46] Bruker, SMART and SAINT, Area Detector Control and Integration Software, Bruker Analytical X-ray Instruments Inc., Madison, Wisconsin, USA, 1997.
[47] G.M. Sheldrick, Acta Crystallogr., Sect. A 64 (2008) 112.
[48] A. Altomare, G. Cascarano, C. Giacovazzo, A. Guagliardi, J. Appl. Crystallogr. 26 (1993) 343.
[49] G.M. Sheldrick, SHELXL-97, Program for the Refinement of Crystal Structures, University of Goettingen, Germany, 1997.
[50] J.E. Huheey, E.A. Keiter, R.L. Keiter, Inorganic Principals of Structure and reactivity, fourth ed., Harper Collins College Publishers, New York, 1993.
[51] L. Pauling, The Nature of the Chemical Bond, third ed., Cornell University Press, New York, 1960.